Effect of Danggui Buxue decoction on hypoxia-induced injury of retinal Müller cells *in vitro*

Xilin Ge,[1,2]* Caoxin Huang,[1]* Wenting Chen,[3] Chen Yang,[3] Wenfang Huang,[3] Jia Li,[3] Shuyu Yang[4,5]

[1]Diabetes Research Institute, The First Affiliated Hospital of Xiamen University, School of Medicine, Xiamen University, Xiamen
[2]Geriatric Department, Zhongshan Hospital (Xiamen), Fudan University, Xiamen
[3]Diabetes Research Institute, The First Affiliated Hospital of Xiamen University, Xiamen
[4]Traditional Chinese Medicine Studio, The First Affiliated Hospital of Xiamen University, Xiamen
[5]Integrated Traditional Chinese and Western Medicine Center, School of Medicine, Xiamen University, Xiamen, China

These authors contributed equally to this work

ABSTRACT

Retinopathy is a common complication of diabetes mellitus and the leading cause of visual impairment. Danggui Buxue decoction (RRP) has been used as a traditional drug for the treatment of diabetic nephropathy for many years. The aim of this study was to investigate the effects of RRP on hypoxia-induced retinal Müller cell injury. A model of retinal Müller cell damage was created using high glucose levels (25 mmol/L) and/or exposure to low oxygen conditions (1% O_2). RRP was given to rats by continuous gavage for 7 days to obtain drug-containing serum. After sterilization, the serum was added to the culture medium at a ratio of 10%. Cell viability, apoptosis, and cell proliferation were assessed using the CCK-8 kit, Annexin V-FITC/propidium iodide apoptosis kit, and EdU kit. The mRNA levels of angiogenesis factors (ANGPTL4, VEGF) and inflammatory factors (IL-1B, ICAM-1) were detected by RT-qPCR. Western blot analysis was employed to assess the levels of proteins related to the ATF4/CHOP pathway. Following hypoxia for 48 h and 72 h, there was a significant decrease in cell viability and proliferation, as well as a notable increase in apoptosis compared to the control group (21% O_2). However, high glucose stimulation had no significant effect, and high glucose combined with hypoxia had no further damage to cells. After 48 h of exposure to low oxygen levels, the mRNA expression levels of ANGPTL4, VEGF, IL-1B, and ICAM-1 in retinal Müller cells were significantly higher than in the control group (21% O_2). RRP treatment significantly alleviated the increase of cell apoptosis and the upregulation of IL-1B and-1 in retinal Müller cells induced by hypoxia. RRP has the potential to reduce the suppression of the ATF4/CHOP pathway in hypoxia-induced retinal Müller cells, and it significantly alleviates cell apoptosis through regulating inflammatory factors and the ATF4/CHOP pathway.

Key words: Danggui Buxue decoction; hypoxia; retinal Müller cells; diabetic retinopathy; ATF4/CHOP pathway.

Correspondence: Shuyu Yang, MD, Traditional Chinese Medicine Studio, The First Affiliated Hospital of Xiamen University, No. 55 Zhenhai Road, Xiamen 361003, China. E-mail: gexilin@aliyun.com

Contributions: all the authors made a substantive intellectual contribution, read and approved the final version of the manuscript and agreed to be accountable for all aspects of the work.

Conflict of interests: the authors declare that they have no competing interests, and all authors confirm accuracy.

Ethics approval: this study was approved by the Ethics Committee of Xiamen University (no. XMU-2-202006-005).

Availability of data and materials: the data used to support the findings of this study are available from the corresponding author upon reasonable request.

Funding: none.

Introduction

According to statistics from the World Health Organization, approximately 422 million people worldwide are affected by diabetes (DM).[1] This phenomenon is mainly due to the sedentary lifestyle and obesity prevalent in modern society. Additionally, approximately 1.5 million deaths each year can be directly linked to diabetes.[2] The rise in DM cases has resulted in a higher occurrence of chronic diabetic issues, including retinopathy, kidney disease, and neuropathy.[3] Compared to other ocular complications associated with diabetes (such as fluctuations in vision, cataracts, and glaucoma), diabetic retinopathy is the primary reason for visual impairment, with a greater frequency and increased risk.[3] Diabetic retinopathy is caused by a complex interplay of factors that are not only related to eye health but also involve overall health status. [4] Elevated levels of blood sugar disrupt the delicate metabolic balance in the retina and diminish the activity of insulin receptors, which are crucial for the growth, development, and survival of neurons, ultimately leading to neuronal apoptosis.[5] Furthermore, elevated levels of oxidative stress, inflammation, diminished neuroprotective factors, and glutamate excitotoxicity are all factors that play a role in the onset of neurodegenerative disorders.[6-8]

The process of apoptosis is regulated by multiple signaling pathways that can either facilitate or suppress the sequence of events culminating in apoptosis.[9] In addition to signaling pathways related to death receptors and mitochondria, endoplasmic reticulum (ER) stress is also widely considered to be an important factor in initiating cell apoptosis signal transduction.[10] Recent studies have shown that ER stress-induced cell apoptosis is closely related to many human diseases, such as diabetes and certain hereditary neurological disorders.[11] Numerous studies have shown that stress in ER is significantly involved in the apoptosis and death of retinal cells, particularly in conditions like age-related macular degeneration and diabetic retinopathy.[9] Heightened ER stress results in inflammatory responses and vascular impairment in diabetic and ischemia-induced retinopathy.[12] In cultured retinal cells, we detected stress in the ER affecting various cell types such as vascular endothelial cells, pericytes, ganglion cells, and Müller cells. Additionally, comparable observations were made in retinal pigment epithelial cells and different animal models of disease.[9] Chronic or intense ER stress may cause a sustained expression of activating transcription factor 4 (ATF4), which in turn enhances the activation of genes that promote apoptosis. Transcription factor C/EBP homologous protein (CHOP) has garnered widespread attention for its ability to promote cell apoptosis, with its expression level primarily regulated by ATF4.[13] CHOP, which is also referred to as growth arrest and DNA damage-inducible gene 153, is crucial in the mechanism of cell apoptosis triggered by ER stress.[14] Studies have shown that ER stress triggers the PERK-ATF4-CHOP signaling pathway, which contributes to ischemia-reperfusion injury (IRI) and apoptosis of R28 cells in the retina, ultimately leading to glaucoma-related pathological issues.[15]

The dysfunction of Müller cells is associated with many retinal diseases, including digital radiography (DR).[16,17] Increasing evidence indicates that in individuals with diabetes mellitus and streptozotocin (STZ) induced diabetes rat, the apoptosis of retinal Müller cells occurs before any changes in retinal microvasculature.[16-18] In the retina, the existence of STZ may aggravate the metabolic and vascular changes caused by diabetes, and then lead to or aggravate the hypoxic state of the retina.

The Danggui Buxue decoction (RRP) is a traditional herbal remedy containing *Angelicae sinensis* radix (Danggui) and *Astragali* radix (Huangqi), which serves to nourish the body's blood and Qi (vital energy).[19] The RRP has been used for many years as a traditional remedy to manage diabetic nephropathy.[20] Some researchers have pointed out that RRP may slow down the progression of diabetic neuropathy induced by STZ and inhibit the accumulation of extracellular matrix within and outside the mesangial cells.[21] RRP suppresses the growth of glomerular mesangial cells caused by elevated glucose levels and decreases the buildup of extracellular matrix.[22] However, it is still unclear whether RRP has the ability to alleviate the damage to retinal Müller cells caused by hypoxia. Therefore, our aim is to examine the effects of RRP on hypoxia-induced injury to retinal Müller cells and its associated mechanisms.

Materials and Methods

RRP source

The RRP decoction in brown color was obtained from the preparation center located at the First Affiliated Hospital of Xiamen University in China. The drug components include *Astragalus membranaceus*, *Angelica sinensis*, and *Panax notoginseng* (ratio of 1:5:1), and the concentration is 1.165 g/L.

Animals, treatment, and preparation of medicated serum

This research followed the National Institutes of Health's Guidelines for the Care and Use of Laboratory Animals, with all experimental procedures compliant with the relevant provisions of the Animal Welfare Act. The project received approval from the Ethics Committee of Xiamen University (XMU-2-202006-005), allowing it to proceed with animal experiments. Sprague-Dawley (SD) rats used in this study were sourced from Shanghai Saike Experimental Animal Co., Ltd. (China), weighing between 350 and 500 g. The rats were kept in the Experimental Animal Center at Xiamen University, where the temperature was regulated between 20 and 23°C, relative humidity ranged from 55 to 70%, and a light-dark cycle of 12 h was followed. The facility adhered to Specific Pathogen-Free (SPF) criteria. After a week of adapting to their new diet, the rats were randomly divided into two groups, each containing three individuals: one group received an oral gavage of RRP at a dosage of 4 g/kg of body weight daily, while the control group was given an equivalent volume of water. This intragastric administration continued for seven days to ensure that blood concentrations reached a stable peak. Blood samples were taken from the abdominal aorta two h after the final gavage on day seven. The serum was obtained by centrifuging at 3000 RPM for 15 min, and after inactivating it at 56°C for 30 min, it was stored at -20°C.

Cell culture and hypoxia induction

These MIO-M1 cells were derived from retinal Müller stem cells obtained from ATCC in Manassas, Virginia. The cells were cultured in DMEM modified for low glucose (DMEM-LG) sourced from Thermo Fisher Scientific (Waltham, MA, USA), supplemented with 10% fetal bovine serum (FBS) procured from Shanghai Shangjing Biotechnology Co., Ltd. (Shanghai, China). The culture environment was maintained at 50% relative humidity, 5% CO2 concentration, and a temperature of 37°C. The cells were divided into four distinct treatment groups. The first group served as the vehicle control (vec) and received an equal volume of the solvent used to dissolve RRP, TM, and TUDCA. The second group received treatment with RRP at a final concentration of 1.165 g/L. To prepare the drug-containing serum for this group, RRP was continuously administered to rats *via* gavage for 7 consecutive days. The third group was exposed to low glucose conditions with 5

mmol/L D-glucose (LG) as a control. This was achieved by adding D-glucose to the cell culture medium to reach the desired concentration. The fourth group was subjected to high glucose conditions with 25 mmol/L D-glucose (HG). Following treatment with high-glucose DMEM or drug-enriched serum, all cells were cultured for a standardized period of 2 h in a normoxic atmosphere of 21% oxygen. Subsequently, all cells, except the normoxic control, were incubated under hypoxic conditions of 1% O2 for 48 h to induce hypoxia. For ER stress induction, the Tunicamycin ™ group was treated with 2.5 μg/mL TM for the first 16 h of hypoxia, while the TUDCA group, serving as the ER stress inhibitor, was treated with 50 μM Tauroursodeoxycholic acid (TUDCA) starting 12 h before the hypoxia exposure.[23] These concentrations and timings were chosen based on prior optimization experiments and are consistent with the data presented in the "Results" section.

MIO-M1 cells were subjected to hypoxia treatment at varying durations to determine the effect of low oxygen conditions on cell behavior. Cells were exposed to 1% O_2 in a hypoxia chamber for 2, 8, 16, 24, 48, and 72 h. At each time point, cells were harvested for further analysis.

Double immunofluorescence staining

For double immunofluorescence staining, MIO-M1 cells were fixed with 4% paraformaldehyde (PFA) in phosphate-buffered saline (PBS) for 15 min at room temperature. Following fixation, cells were permeabilized with 0.1% Triton X-100 in PBS for 10 min to enhance antibody penetration.

After permeabilization, non-specific binding was blocked by incubating the cells with 3% bovine serum albumin (BSA) in PBS for 1 h at room temperature. The primary antibodies, rabbit anti-glutamine synthetase (GS) and mouse anti-cell retinal binding protein (CRALBP), were diluted in blocking buffer and applied to the cells overnight at 4°C in a humidified chamber.

The next day, cells were washed three times with PBS to remove unbound primary antibodies and then incubated with the appropriate secondary antibodies conjugated to fluorophores (such as Alexa Fluor 488 for rabbit IgG and Alexa Fluor 594 for mouse IgG) diluted in blocking buffer (1:500) for 1 h at room temperature in the dark.

After incubation with secondary antibodies, cells were washed again with PBS and the cell nuclei were counterstained with Hoechst 33342 (1 μg/mL) for 5 min at room temperature. Finally, the cells were washed with PBS, and the fluorescence signals were visualized using a fluorescence microscope. The following primary and secondary antibodies were used: Rabbit anti-GS (PA5-28940, 1:100; Invitrogen, Waltham, MA, USA); Mouse anti-CRALBP (MA1-813, 1:100; Invitrogen); Donkey anti-rabbit IgG conjugated with Alexa Fluor 488 (A-21206, 2 μg/mL; Invitrogen); Goat anti-mouse IgG conjugated with Alexa Fluor 594 (A-11005, 2 μg/mL; Invitrogen). Fluorescence images were captured using a confocal microscope (Œ., LSM 880; Zeiss, Oberkochen, Germany) with a 63x oil immersion objective. The excitation/emission wavelengths for Alexa Fluor 488 and Alexa Fluor 594 were 495/519 nm and 590/617 nm, respectively. Hoechst 33342 was excited at 350/365 nm and emitted at 455/510 nm. Images were analyzed using imaging software (*e.g.*, Zen Blue, Zeiss) to quantify fluorescence intensity and co-localization as indicated. Negative controls were conducted by excluding the primary antibody and substituting it with PBS.

CCK-8 assay

Cell viability was assessed utilizing the CCK-8 assay kit provided by Beijing Solarbio Biotechnology Co., Ltd. (Beijing, China). Initially, MIO-M1 cells in the logarithmic growth phase were seeded at a density of 5,000 cells per well within a 96-well plate. Following cell adhesion to the plate surface, treatments were applied according to established protocols and incubated for a duration of 48 h. Afterward, 10 mL of CCK-8 solution was introduced into each well and incubated at 37°C under appropriate humidity conditions for 1 h. The absorbance was subsequently measured at 450 nm using a microplate reader.

EdU assay

The Cell-Light™ EdU Apollo488 *ex vivo* kit produced by RIBBIO Co., Ltd. (Guangzhou, China) was employed to evaluate cell proliferation. Therefore, to evaluate cell proliferation, MIO-M1 cells were plated in 96-well plates at a density of 5,000 cells per well. They were then fixed with 4% formaldehyde at room temperature for approximately 30 min. Subsequently, a solution of glutamate (2 mg/mL) was added and gently agitated for 5 min. After that, Triton X-100 (0.5%) was introduced and incubated for an additional 10 min to enhance cellular membrane permeability. The staining solution was then applied to the samples and incubated in darkness at room temperature for 30 min. Upon completion of this step, Hoechst 33342 solution (at a concentration of 1 μg/mL) was added and further incubated in darkness for another 30 min. Finally, cellular observations and analyses were conducted using a Nikon fluorescence microscope. We evaluate the cell proliferation rate by quantifying the number of EdU-positive cells relative to the total cell count.

Cell apoptosis detection

Cell apoptosis was quantified utilizing a kit from Nanjing Jiancheng Biological Engineering Research Institute (China). Following a 48-h incubation period, cells were dissociated from the culture flask using trypsin and subsequently transferred into 10 mL centrifuge tubes. The cell suspension underwent centrifugation at 1,000 rpm for 5 min, after which the supernatant was discarded. The resultant cell pellet, containing approximately 1×10^6 cells per sample, was resuspended in 500 mL of binding buffer. Subsequently, 5 mL of Annexin V-FITC/propidium iodide (PI) reagent was introduced and gently mixed, followed by the addition of 5 mL of PI, which was also mixed with care. This solution was incubated in darkness at ambient temperature for 10 min. Ultimately, flow cytometric analysis (ACEA Biosciences) was conducted, wherein Annexin V-FITC emitted green fluorescence and PI exhibited red fluorescence.

Western blot

After 48 h of culture, the cells were lysed using cooled RIPA buffer (provided by Shanghai Baiyuntian Biotechnology Co., Ltd., Shanghai, China), and the resulting lysate was obtained from Shanghai Sheneng Biotechnology Co., Ltd. (Shanghai, China). Subsequently, a 100-fold concentrated mixture of proteinase and phosphatase inhibitors (Shanghai Sheneng Biotechnology Co., Ltd.) was added. We then centrifuged the protein sample at 13,000 rpm for 20 min at 4°C to extract the sample. We then used an improved version of the BCA assay kit to determine the protein concentration. (manufactured by Shanghai Baiyuntian Biotechnology Co., Ltd., Shanghai, China). We commenced by isolating 50 micrograms of protein via SDS-PAGE, subsequently transferring the proteins onto a PVDF membrane. To effectively block nonspecific binding sites on the membrane at ambient temperature for approximately 1 h, we utilized either non-fat dry milk or BSA procured from Shanghai Sheneng Biotechnology Co., Ltd. Following this blocking procedure, the primary antibody was incubated overnight at 4°C, after which the secondary antibody was applied at room temperature for an additional hour. Ultimately, we employed the Minichemi™ 610 Chemical Imaging System located in Beijing to visualize and

analyze the protein bands, obtaining optical density measurements from three independent replicates using ImageJ software.

The primary antibodies and secondary antibody used in this study were listed as follows: Mouse anti-VEGF (MA5-13182, 1.5 µg/mL; Invitrogen); Mouse anti-PCNA (13-3900, 0.5 µg/mL; Invitrogen); Rabbit anti-ATF4 antibody (MA5-32364, 1:1,000; Invitrogen); Mouse anti-CHOP antibody (MA1-250, 1:1,000; Invitrogen); Rabbit anti-β-actin antibody (ab8227, 1:5,000; Abcam, Cambridge, UK); Goat anti-rabbit IgG HRP-conjugated antibody (AP307P, 1:10,000; Sigma-Aldrich, St. Louis, MO, USA); Goat anti-mouse IgG HRP-conjugated antibody (12-349, 1:10,000; Sigma-Aldrich).

RT-qPCR

We extracted total RNA from MIO-M1 cells using reagents from Beijing Tiangen Biotechnology Co., Ltd. (Beijing, China). Then, we used the FastQuant cDNA Synthesis Kit from the same company to turn 1 microgram of RNA into complementary DNA (cDNA). Subsequently, we executed quantitative reverse transcription polymerase chain reaction on the Bio-Rad CFX96 platform utilizing SYBR Green PCR Master Mix supplied by TianGen Biotechnology Co., Ltd. The amplification protocol encompassed the following phases: an initial denaturation at 95°C for 15 s, annealing at 65°C for 20 s, and extension at 72°C for 15 s. This cycle was performed a total of 40 iterations, with β-actin serving as an internal reference gene. To evaluate relative alterations in target gene expression levels, we employed the $2^{-\Delta\Delta CT}$ methodology. Comprehensive primer sequences are detailed in Table 1.

Statistical analysis

Statistical analysis was performed using GraphPad Prism 5 software in La Jolla, California. Results were presented as the average value ± SD of multiple samples or at least three technical replicates. We compared different groups using one-way analysis of variance (ANOVA) and assessed differences between groups using Kruskal-Wallis test if the homogeneity and normality assumptions were met. When *p*-value was less than 0.05, it indicated statistically significant differences between groups.

Results

Retinal Müller cell line MIO-M1 injury model

MIO-M1 cells were identified by double immunofluorescence staining, and the marker proteins were GS and CRALBP. The nuclei were labeled with Hoechst 33342 dye, while the cells were identified using rabbit anti-GS antibody and mouse anti-CRALBP antibody (Figure 1A). The pathological environment of diabetic retina was simulated by high glucose and/or hypoxia stimulation. Experiments were conducted on MIO-M1 cells under varying durations of hypoxic treatment, specifically at 2, 8, 16, 24, 48, and 72 h. Investigations have demonstrated that the mRNA and protein expression levels of vascular endothelial growth factor (VEGF) and angiopoietin-like factor 4 (Angptl4) in MIO-M1 cells are markedly elevated in the hypoxia-induced group relative to the control cohort (Figure 1 B,D). This observation substantiates that a hypoxic model has been successfully developed within the context of this research.

Hypoxia inhibited the cell viability and cell proliferation of MIO-M1 cells

In our investigation, we assessed the effects of elevated glucose concentrations (25 mmol/L) and hypoxic conditions (1% O_2) on MIO-M1 cells. The CCK-8 assay was employed to quantify cell viability. Our results demonstrated a marked decline in cell viability relative to the control group (21% O_2) following 48 h (Figure 2A; p=0.0009) and 72 h (Figure 2B; p=0.0087) of hypoxic exposure. Conversely, no statistically significant variations in cell viability were detected under high-glucose conditions at these time points. Compared with hypoxia stimulation, high glucose combined with hypoxia had no further injury to MIO-M1 cells (Figure 2 A,B). Next, we further detected cell proliferation by EdU kit and PCNA protein expression. After being cultured in low oxygen environment for 48 h, the cell proliferation was significantly lower than that of the control group (21% O_2, p=0.032; Figure 2 C,D). Similarly, high glucose stimulation did not have a significant impact on cell proliferation, and the combination of high glucose with hypoxia did not lead to any further harm to the cells (Figure 2 C,D). Under hypoxic conditions, the expression levels of PCNA protein were significantly diminished compared to the control group (21% O_2), particularly at 24, 48, and 72 h following hypoxia exposure. This observation further supports the notion that hypoxia is implicated in attenuating cellular proliferation (Figure 2E).

Hypoxia promoted apoptosis of MIO-M1 cells

We investigated the apoptosis of MIO-M1 cells under hypoxic conditions (1% oxygen) and elevated glucose concentrations (25 mmol/L) through Annexin V/PI staining in conjunction with flow cytometric analysis. The results are depicted in a representative scatter plot of MIO-M1 cells, along with their quantitative assessment (Figure 3). A significantly increased proportion of Annexin V-positive cells was observed in the hypoxia treatment group relative to the control cohort, particularly after 48 h of low oxygen exposure (p<0.001; Figure 3). This suggests a marked induction of apoptosis in MIO-M1 cells following both 24 and 48 h under hypoxic stress. Conversely, high glucose conditions did not induce significant alterations in apoptosis levels relative to the control group (21% O_2). Additionally, no further cellular damage was observed when high glucose and low oxygen were combined (Figure 3).

Table 1. The primer sequences.

Genes (human)	Forward primers Reverse primers
β-actin	CAGCCTTCCTTCCTGGGCATGATTGTGCTGGGTGCCAGGGCAG
VEGF	TCAAGCCATCCTGTGTGCCGGCCTTGGTGAGGTTTGATCC
IL-1β	AGCTACGAATCTCCGACCACCGTIATCCCATGTGTCGAAGAA
Angpt14	CTTGGGACCAGGATCACGACAAACCACCAGCCTCCAGAGAG
ICAM-1	AGGGTAAGGTTCTTGCCCACTGATGGGCAGTCAACAGCTA
CHOP	TGAGGAGAGAGTGTTCAAGAAGGGGAGTGGCTGGAACAAGCTC
ATF4	TCCAACAACAGCAAGGAGGATGTCATCCAACGTGGTCAGAAGG

Hypoxia promoted the expression of angiogenesis factors and inflammatory factors in MIO-M1 cells

In diabetes mellitus, there is a marked upregulation of pro-inflammatory cytokines within the retinal environment, including VEGF and intercellular adhesion molecule-1 (ICAM-1). During the early phases of diabetic retinopathy, retinal capillary endothelial cells become activated and secrete considerable quantities of these inflammatory mediators. Consequently, our objective was to assess the levels of these inflammatory mediators. Following a thorough analysis across various experimental time points, we opted for a 48-h hypoxic treatment to facilitate further investigation. In MIO-M1 cells, hypoxic conditions resulted in a significant upregulation of mRNA expression levels for Angptl, VEGF (21% O_2, p=0.0003; Figure 4A), IL-1β (21% O_2, p=0.0017; Figure 4D), and ICAM-1 (21% O_2, p=0.0033; Figure 4A) when contrasted with the control group.

RRP did not affect the decrease of cell viability and proliferation of MIO-M1 cells induced by hypoxia

To investigate the influence of RRP on the viability of MIO-M1 cells under hypoxic conditions, we conducted a CCK-8 assay to quantify cell survival. The data revealed that after 48 h of

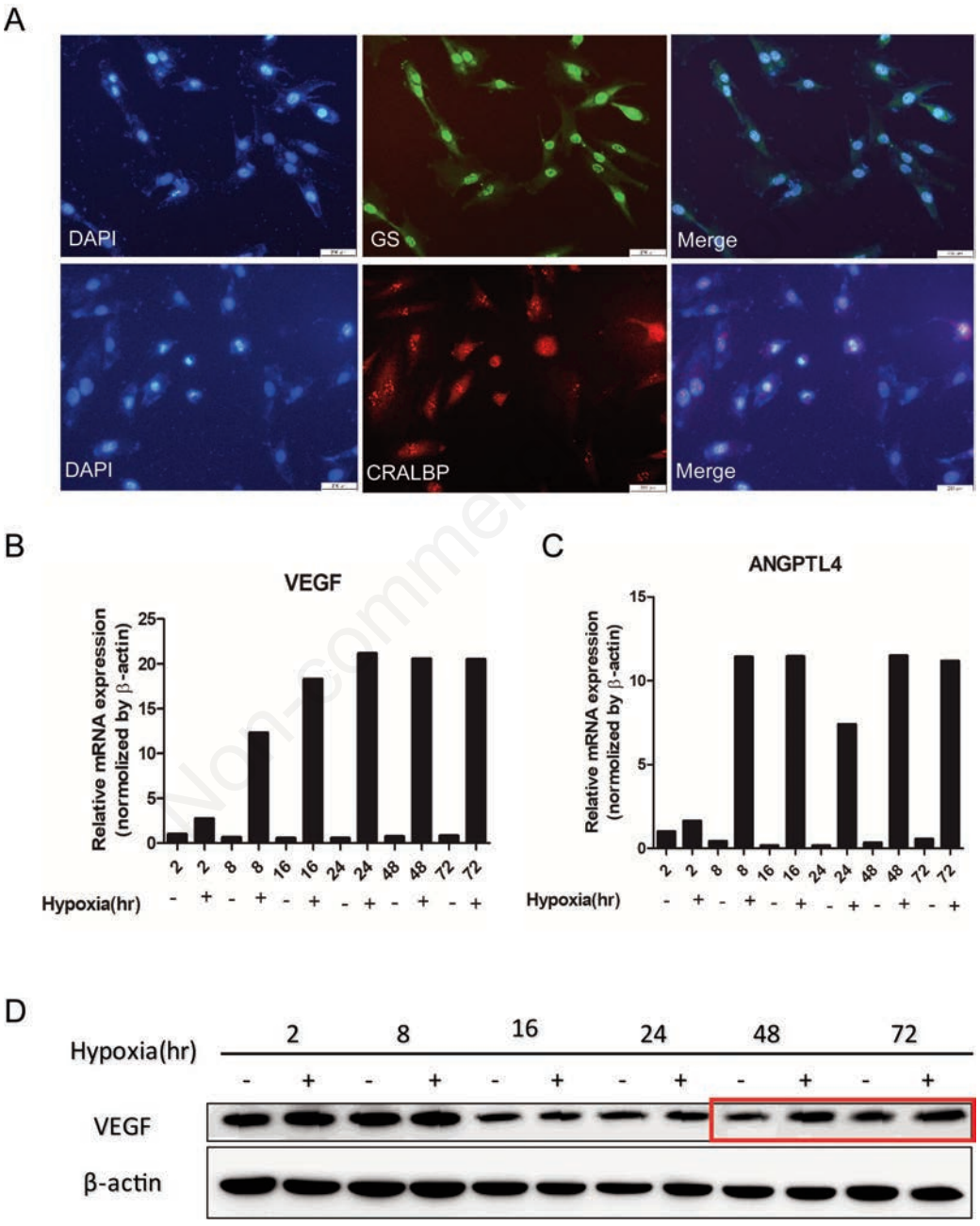

Figure 1. The expression levels of glutamine synthetase (GS), cell retinal binding protein (CRALBP), vascular endothelial growth factor (VEGF), and angiopoietin-like factor 4 (Angptl 4) induced hypoxia. **A**) GA and CRALBP expression levels by immunofluorescence staining; scale bar: 200 μm. **B,C**) VEGF and Angptl4 mRNA expression levels by RT-qPCR. **D**) VEGF protein expression level by Western blot.

hypoxia, the survival rate of MIO-M1 cells was significantly diminished compared to the control group (vec group), with statistical significance (p=0.0410). However, RRP did not yield a statistically significant enhancement in this context (Figure 5A). Subsequently, we employed EdU staining to further analyze MIO-M1 cell proliferation. The results demonstrated a pronounced reduction in proliferative capacity within the hypoxic environment relative to the control group (vec group) (p=0.0058). Nevertheless, RRP did not exhibit any substantial effect on cellular proliferation when assessed against hypoxic conditions (Figure 5 B,D).

RRP effectively alleviated the increase of MIO-M1 cell apoptosis caused by hypoxia

To conduct a thorough evaluation of the apoptosis status of MIO-M1 cells, we employed Annexin V/PI staining combined with flow cytometry for comprehensive analysis. After 48 h of hypoxic treatment, the MIO-M1 cell population exhibited a significantly elevated proportion of Annexin V-positive cells compared to the control group (21% O_2; Figure 6). Moreover, subsequent to RRP administration, the incidence of Annexin V-positive cells in the RRP-treated cohort was markedly diminished relative to that

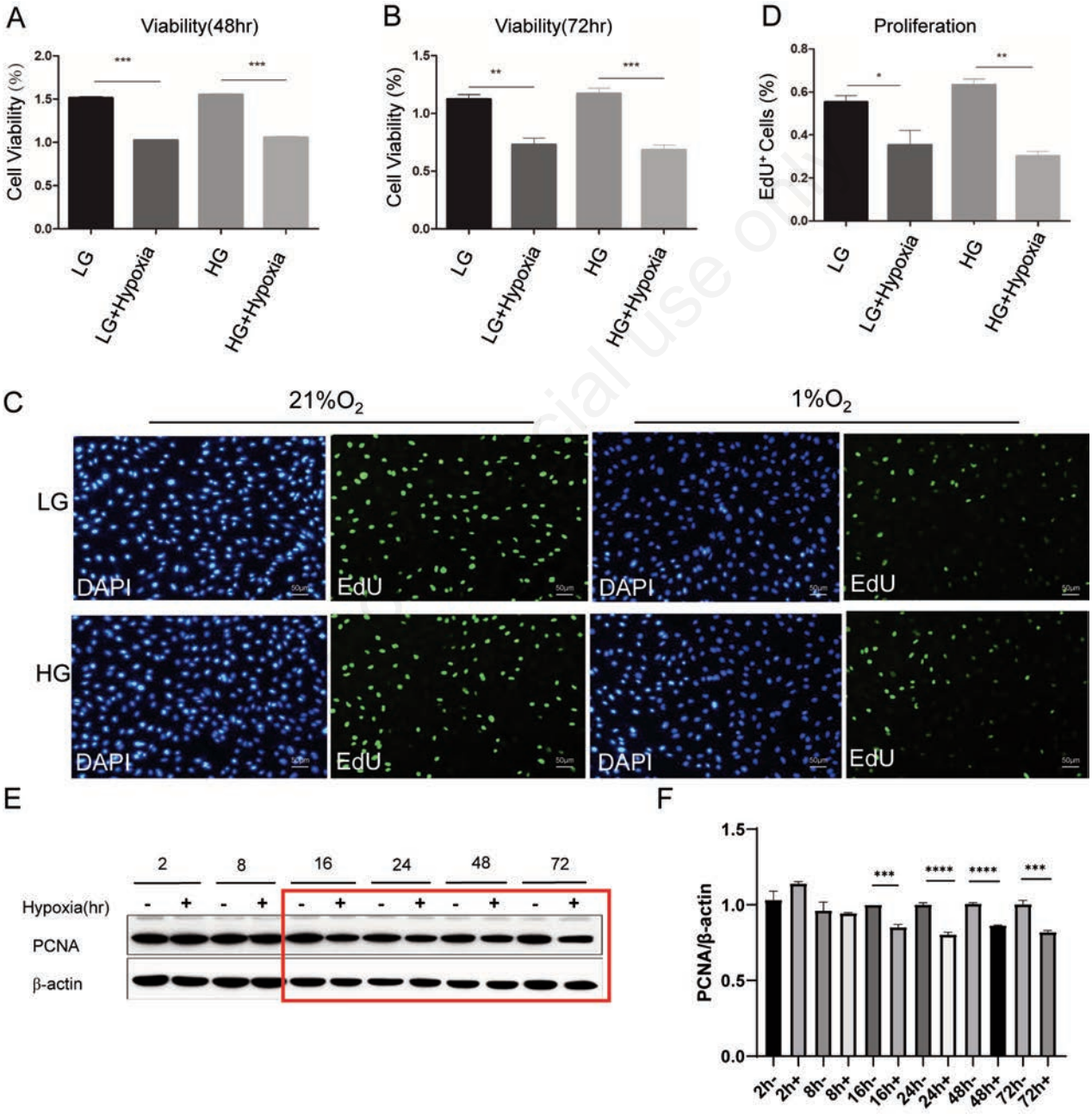

Figure 2. Cell viability, cell proliferation, and PCNA expression level induced hypoxia and high glucose. **A,B**) cell viability with stimulation of hypoxia and high glucose for 48 h and 72 h. **C,D**) Cell proliferation with stimulation of hypoxia and high glucose by EdU assay and quantitative analysis; scale bar: **C**) 50 μm. **E**) PCNA protein expression with stimulation of hypoxia and high glucose by western blot. *p<0.05; **p<0.01; ***p<0.001.

observed in the control group (vec group; Figure 6), indicating that RRP demonstrates a substantial efficacy in mitigating apoptosis induced by hypoxia in MIO-M1 cells.

Effect of RRP on the up-regulation of angiogenesis and inflammatory factors in MIO-M1 cells induced by hypoxia

Following a 48-h hypoxic exposure, we observed that the mRNA expression levels of angiogenesis-related factors ANGPTL4 and VEGF in MIO-M1 cells were significantly elevated in the serum control group compared to the treatment group (p=0.003). Conversely, RRP did not exert a statistically significant influence on the expression of ANGPTL4 and VEGF under hypoxic conditions (Figure 7 A,B). Furthermore, sustained hypoxia for 48 h resulted in a marked upregulation of ICAM-1 and IL-1β mRNA levels (p<0.001), whereas RRP effectively attenuated the expression of these two inflammatory mediators (Figure 7 C,D).

RRP alleviated hypoxia-induced apoptosis of MIO-M1 cells through ER stress

To investigate whether the apoptosis of MIO-M1 cells induced by hypoxia was mediated by ER stress, we introduced the ER stress inhibitor, TUDCA. We found that hypoxia-induced apoptosis in MIO-M1 could be significantly blocked by TUDCA (p=0.0038, Figure 8A; p=0.0007, Figure 8B). In addition, after treatment with ER stress agonist, TM, we found that the apoptosis of MIO-M1 cells increased after 48 h of hypoxia was notably increased (p=0.019; Figure 9 C,D). Through these results, we believe that the increase of apoptosis in MIO-M1 cells induced by hypoxia occurs through the ER stress pathway.

RRP mediated hypoxia-induced apoptosis of MIO-M1 cells through the ATF4/CHOP pathway in ER stress

Research has demonstrated that the protective effect of RRP on MIO-M1 cells under hypoxic conditions is intricately linked to the ER stress pathway. To further elucidate this mechanism, we examined the expression levels of key components within this pathway. In comparison to the control cohort (vec), there was a significant upregulation of mRNA expression levels for ATF4 and CHOP following 48 h of hypoxic exposure). Conversely, subsequent administration of RRP led to a substantial downregulation of these gene expressions (p=0.047, Figure 9A; p=0.025, Figure 9 A,B). Similarly, after 48 h under hypoxic conditions, the protein concentrations of ATF4 and CHOP were markedly elevated relative to the control group (21% O_2); however, they exhibited a pronounced reduction following RRP intervention (Figure 9 C,D).

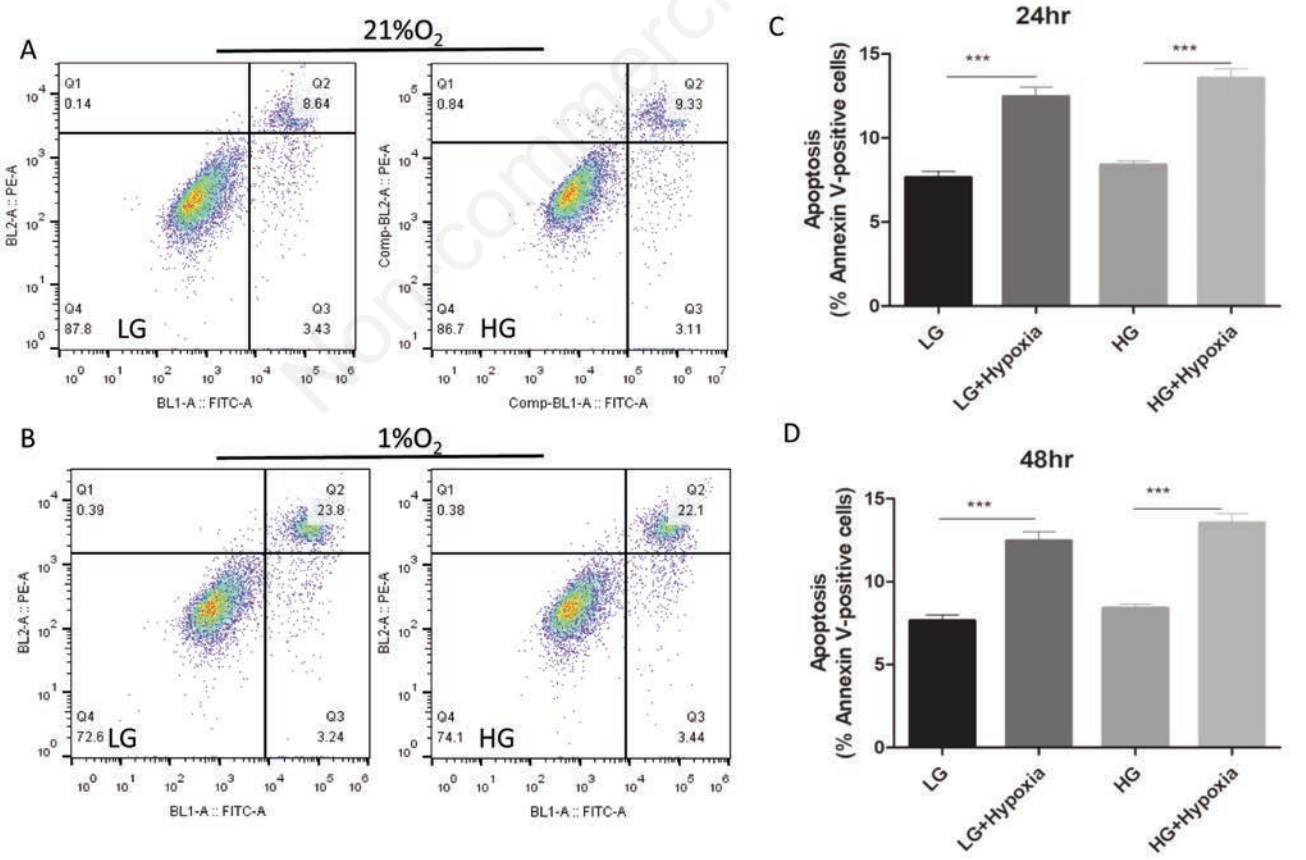

Figure 3. Apoptosis of MIO-M1 cells induced by hypoxia and high glucose using Annexin V/PI staining. **A,C**) apoptosis induced by hypoxia and high glucose for 24 h. **B,D**) apoptosis induced by hypoxia and high glucose stimulation for 48 h. ***p<0.001.

Discussion

The protective effect and potential mechanism of RRP on diabetic retina were further confirmed in this study, offering a new scientific foundation for treating early diabetic retinopathy and using RRP. In this research, we observed a significant increase (almost 20 times) in VEGF expression in retinal Müller cells following hypoxia, particularly at 24 h, 48 h, and 72 h. This finding confirms the pathological changes associated with inflammation and angiogenesis in diabetic retinopathy, contributing to the development of DR. However, our study showed that RRP did not impact the up-regulation of VEGF. This may be due to our use of a short-term (48 h) hypoxia model, which represents the early stage of diabetic retinopathy where RRP may not affect vascular lesions. Additionally, it has been noted that endogenous VEGF plays a role in maintaining and supporting retinal neurons while also serving as a survival factor for photoreceptor cells.[24] It has been documented that the administration of VEGF can also provide protection for retinal ganglion cells (RGCs) in different neurotoxic models.[25] In a different earlier research, the blocking of VEGF in retinas of normal adult resulted in considerable reduction of ganglion cells.[26] Hence, it is crucial to take into account the need for neuroprotection, particularly when treating proliferative diabetic retinopathy with anti-VEGF therapy aimed at reducing neovascularization.[27] This may be another possible reason why RRP does not affect the significant up-regulation of VEGF expression in our study. In our research, RRP has the potential to act as a neuroprotective substance, effectively reducing hypoxia-induced damage in retinal glial cells. This aligns with the known role of VEGF in supporting and maintaining retinal neurons and protecting them from harm. We acknowledge that anti-VEGF therapies are a mainstay in the treatment of DR, particularly in cases with significant neovascularization. These treatments primarily target the vasoproliferative aspects and do not address the neurodegenerative components of the disease. Our study suggests that Danggui Buxue decoction may offer neuroprotection by reducing apoptosis in retinal Müller cells, which is a novel approach compared to the current anti-VEGF strategies. This potential neuroprotective effect of RRP could be particularly beneficial in the context of DR, where neurodegeneration is a key feature.

We used high glucose and hypoxia to simulate the pathological environment of diabetic retina. We observed that following hypoxia, the levels of inflammatory factors ICAM-1 and IL-1β were elevated in retinal Müller cells. Additionally, RRP demonstrated the ability to partially mitigate this upregulation, suggesting its potential to alleviate early diabetic retinal inflammation and improve retinal microcirculation, ultimately preventing DR progression. This is consistent with most previous research results. Müller cells are the predominant type of glial cells fund in the retina, extending across the full thickness of the neuroretina and encircling all retinal neurons.[28] Apart from being close to RGCs, Müller cells are positioned between the vascular system and neurons in the retina.[29] The morphological connection between Müller cells and RGCs plays a crucial role in their

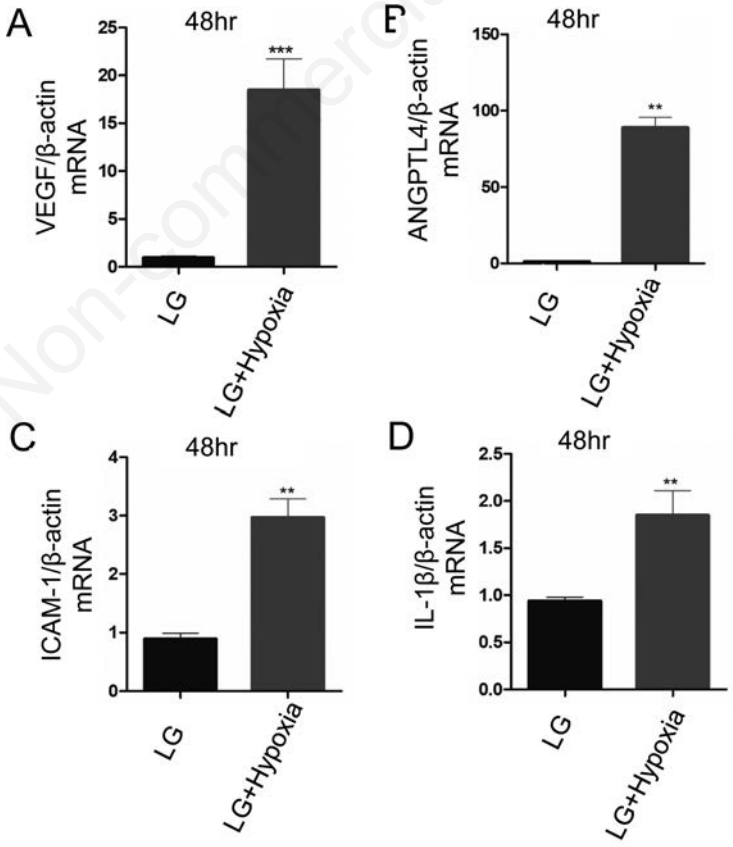

Figure 4. The mRNA expression levels of angiogenesis factors (ANGPTL4, VEGF) and inflammatory factors (IL-1B, ICAM-1) induced by hypoxia and high glucose were detected by qRT-PCR. **A**) VEGF. **B**) ANGPTL4. **C**) ICAM-1. **D**) IL-1β. **$p<0.01$; ***$p<0.001$.

metabolic symbiosis. Recent studies have established the significance of glial cell interaction in the retina, with increasing literature demonstrating the essential role of Müller cells in supporting RGCs.[30,31] In this study, we found that the proportion of apoptotic cells in retinal Müller cells was increased after hypoxia stimulation for 24 to 48 h, which was consistent with the above results. Moreover, we also found that RRP can effectively alleviate the increase of apoptotic retinal Müller cells, to better maintain the function of RGCs. Combined with our previous research results, we believe that RRP can improve diabetic retinal neuropathy, thereby alleviating the disease earlier.

ER stress plays a pivotal role in the apoptosis of rRGCs across diverse contexts.[9,32] In diabetic animal models, Müller cells in the retina show typical markers of ER stress, with significant increases in ATF4 and VEGF levels. Inhibiting ER stress or ATF4 can significantly lower VEGF levels and reduce the expression of inflammation-related genes such as ICAM-1 and TNF-α, effectively alleviating vascular leakage in the diabetic

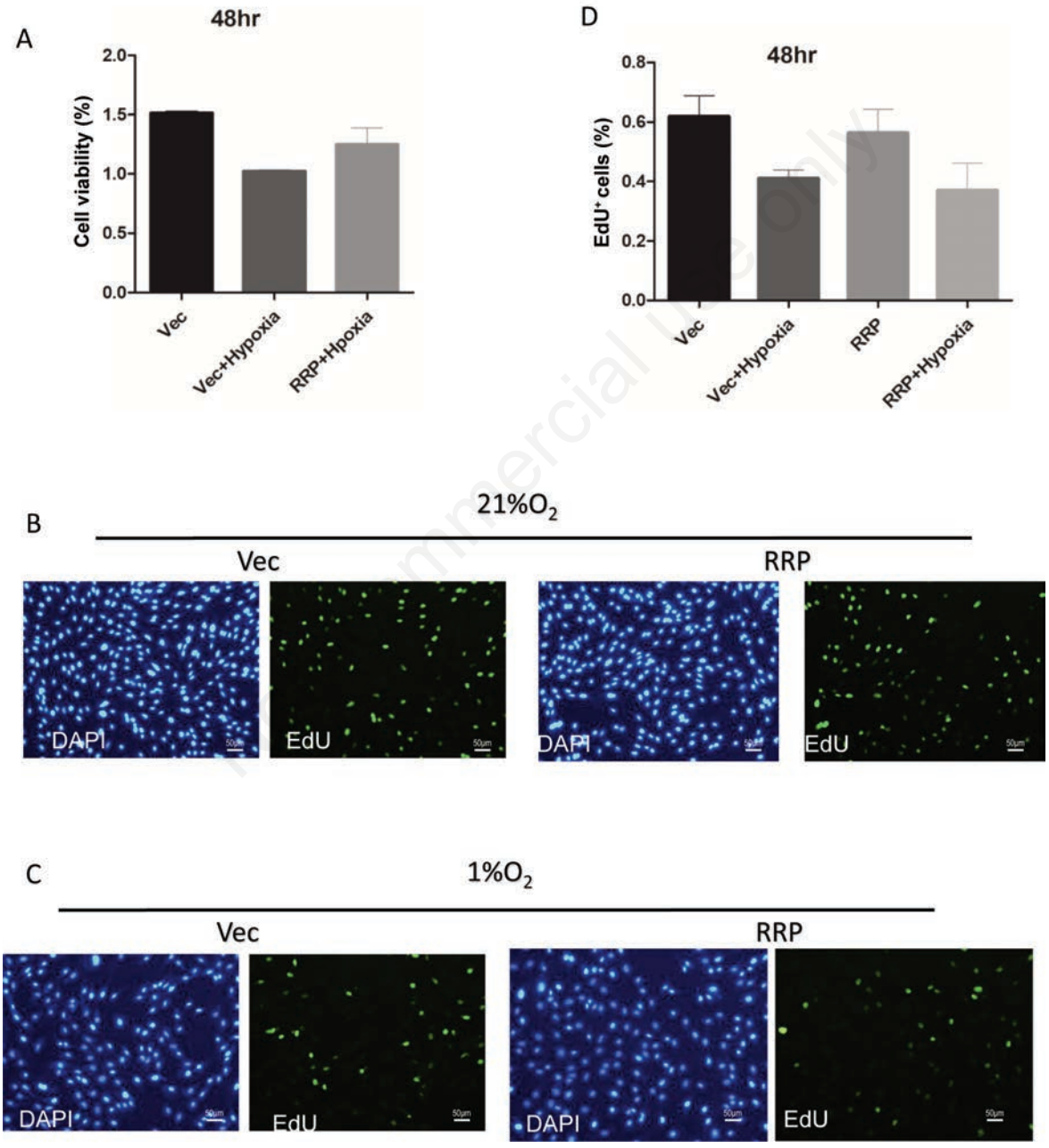

Figure 5. Cell viability and cell proliferation induced by hypoxia and/or Danggui Buxue decoction (RRP). **A**) Cell viability with stimulation of hypoxia and RRP for 48 h. **B**) Cell proliferation with stimulation of RRP by EdU assay. **C**) Cell proliferation with stimulation of hypoxia and/or RRP by EdU assay. Scale bars: 50 μm.

retina.[33] ATF4 is a transcription factor characterized by its high affinity for DNA binding, belonging to a distinct class of regulatory proteins. This class includes notable families such as the activator protein-1 (AP-1) family, cAMP response element-binding protein (CREB), and CREB-like molecules. As a pivotal transcriptional regulator, ATF4 interacts with cAMP response elements located in the promoters of target genes, thereby activating critical gene expression pathways linked to oxidative stress responses, amino acid metabolism, and transport mechanisms. Moreover, ATF4 serves as a principal inducer of C/EBP homologous protein (CHOP), which is recognized as an essential modulator of apoptosis induced by ER stress conditions.[9]

In retinal endothelial cells grown in culture, hypoxia triggers ER stress. Hypoxia effectively promotes inflammation and angiogenesis, but this can be stopped by using chemical chaperones.[9] Therefore, on the other hand, we can also use ER stress inhibitors, such as TUDCA, to block ER stress, thereby alleviating hypoxia-induced retinal injury and inflammatory response in

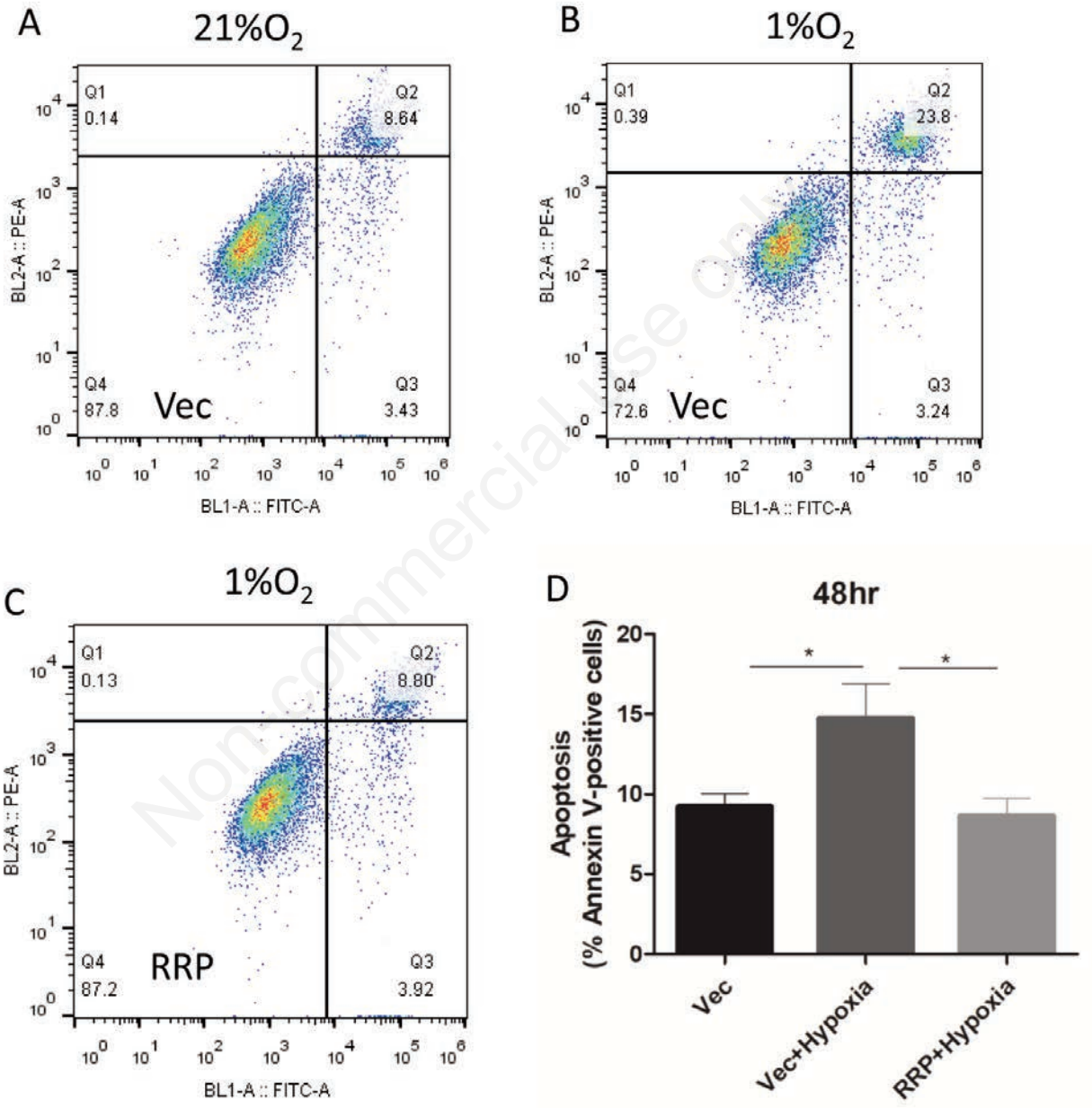

Figure 6. Apoptosis of MIO-M1 cells induced by hypoxia and Danggui Buxue decoction (RRP) using Annexin V/PI staining. **A**) Apoptosis induced by 21% O_2. **B**) Apoptosis induced by 1% O_2. **C**) Apoptosis induced by 1% O and RRP. **D**) quantitative analysis of apoptosis. *p<0.05.

diabetic retinopathy, thereby alleviating DR progression.[23] In our study, after hypoxia, ATF4 and CHOP proteins were upregulated in the ER stress of MIO-M1 cells. The RRP-containing serum effectively alleviated the up-regulation of ATF4 and CHOP. It can be seen that apoptosis is indeed mediated by ATF4 and CHOP. Combined with the application of ER stress agonist, TM, and inhibitor, TUDCA, we can determine that the apoptosis of MIO-M1 cells after hypoxia is mediated by ATF4/CHOP pathway in ER stress, and RRP alleviates apoptosis by inhibiting the expression of factors in ATF4/CHOP pathway. As a result, the identification of important pro-apoptotic and anti-apoptotic pathways in ER stress-induced apoptosis and exploration of their roles in various retinal cell diseases could lead to the development of novel medications for treating retinal disorders. We recognize that our short-term hypoxia model (48 h) may not fully capture the chronic and progressive nature of DR. We discuss how this model primarily represents the early stages of DR and may not reflect the long-term effects of hypoxia and hyperglycemia on retinal cells. To address this limitation, we propose future studies that will extend the duration of hypoxia exposure and include a time-course analysis to better understand the chronic effects on retinal cells. Additionally, we plan to explore the combination of RRP with existing treatments to assess potential synergistic effects in reducing retinal inflammation and neurodegeneration.

In conclusion, hypoxia is one of the key causes of retinal Müller cell injury, and retinal Müller cells are more sensitive to hypoxic (1% O_2) stimulation rather than high glucose. Hypoxia may lead to reduced viability and proliferation of retinal cells, elevated apoptosis, and heightened levels of angiogenesis factors and pro-inflammatory factors. RRP can effectively alleviate the increase of hypoxia-induced apoptosis and alleviate the up-regulation of inflammatory factors to a certain extent. RRP may alleviate hypoxia-induced apoptosis of retinal Müller cells by inhibiting the ATF-4/CHOP pathway in ER stress. This research enhances the understanding of how RRP helps to protect against diabetic retinopathy and highlights the significance of reducing apoptosis and addressing ER stress in the management of diabetic retinopathy.

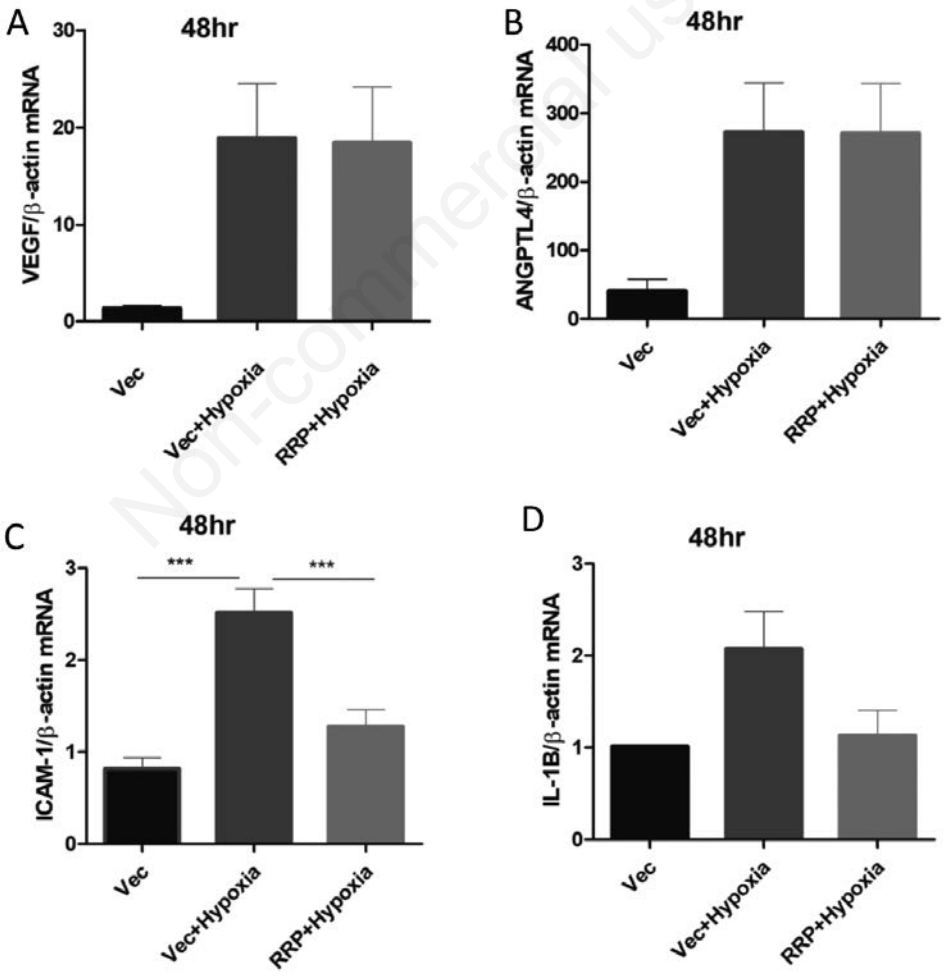

Figure 7. The mRNA expression levels of angiogenesis factors (ANGPTL4, VEGF) and inflammatory factors (IL-1B, ICAM-1) induced by hypoxia and Danggui Buxue decoction were detected by qRT-PCR. (**A**) VEGF; (**B**) ANGPTL4; (**C**) ICAM-1; (**D**) IL-1β. ***p<0.001

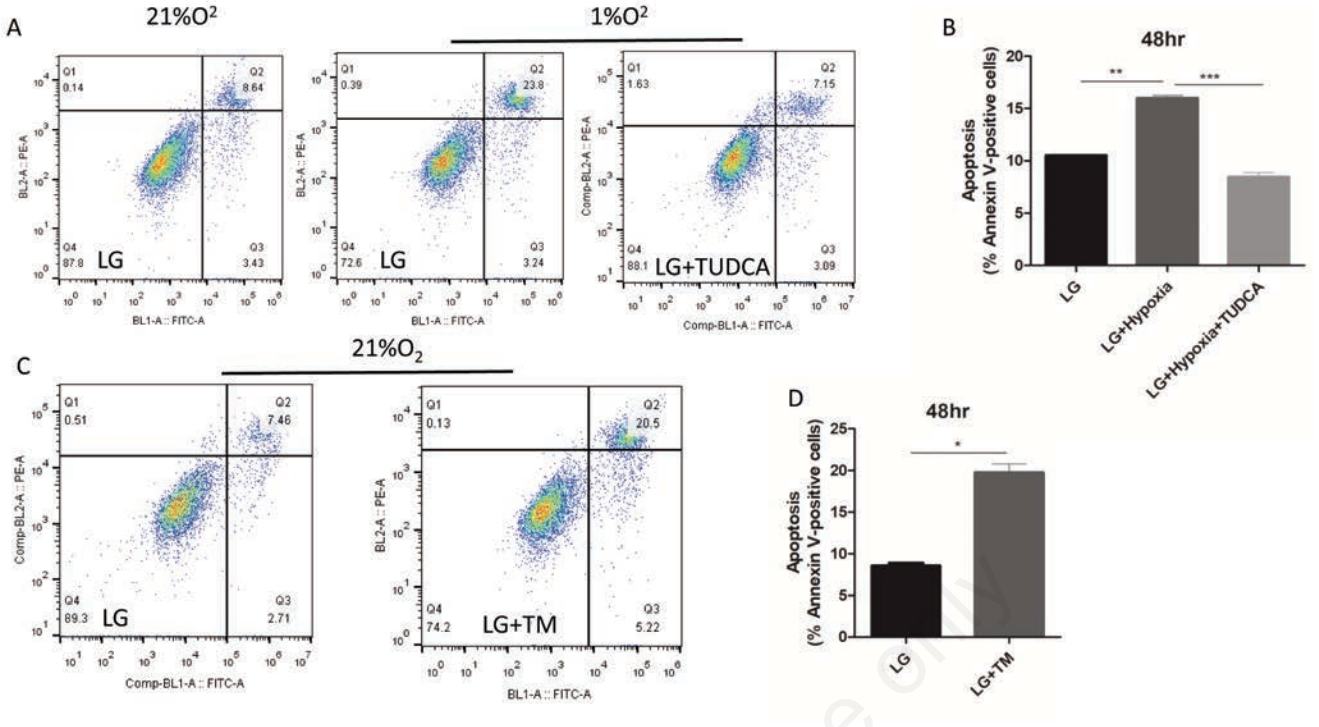

Figure 8. Apoptosis of MIO-M1 cells induced by hypoxia, ER stress inhibitor, and ER stress agonist using Annexin V/PI staining. **A**) Apoptosis induced by 21% O_2, 1% O_2 or TUDCA. **B**) Quantitative analysis of apoptosis induced by TUDCA. **C**) Apoptosis induced by 1% O_2 and Tunicamycin. **D**) Quantitative analysis of apoptosis induced by Tunicamycin. *p<0.05; **p<0.01; ***p<0.001.

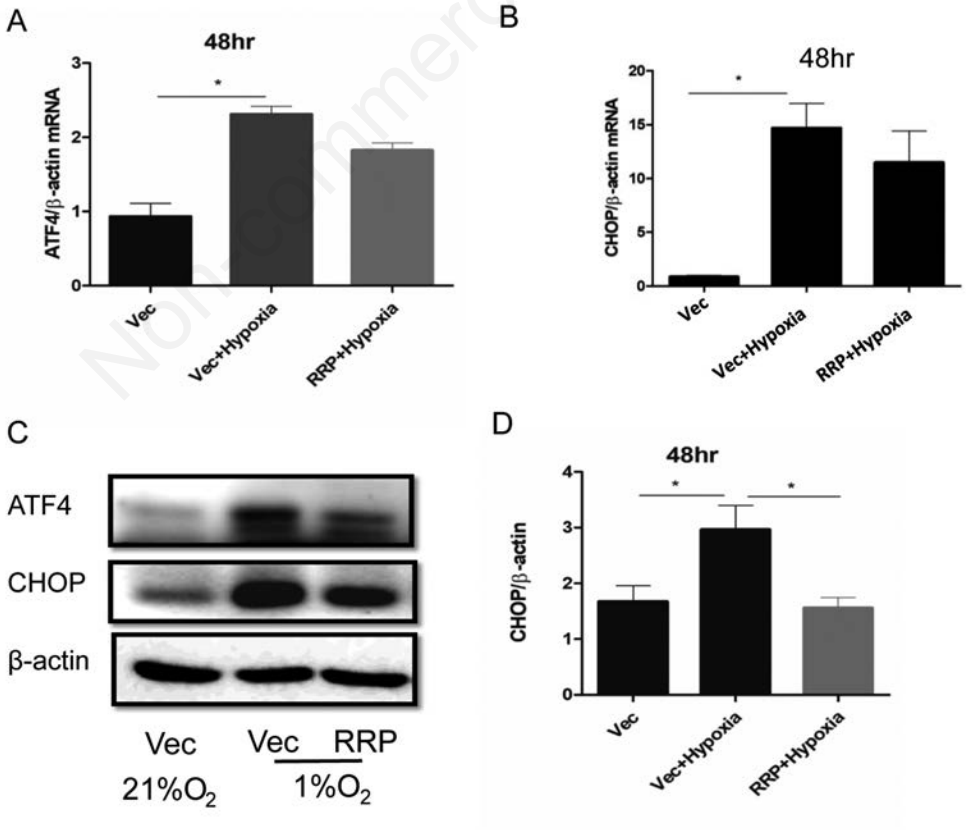

Figure 9. The mRNA and protein expression levels of ATF4 and CHOP in MIO-M1 cells induced by hypoxia and Danggui Buxue decoction. **A,B**) the mRNA expression levels of ATF4 and CHOP. **C,D**) Protein expression levels of ATF4 and CHOP. *p<0.05.

References

1. GBD 2021 Diabetes Collaborators. Global, regional, and national burden of diabetes from 1990 to 2021, with projections of prevalence to 2050: a systematic analysis for the Global Burden of Disease Study 2021. Lancet 2023;402:203-34. Erratum in Lancet 2023;402:1132.
2. Basri NI, Mahdy ZA, Ahmad S, Abdul KA, Shan LP, Abdul MM, et al. The World Health Organization (WHO) versus The International Association of Diabetes and Pregnancy Study Group (IADPSG) diagnostic criteria of gestational diabetes mellitus (GDM) and their associated maternal and neonatal outcomes. Horm Mol Biol Clin I 2018;34:20170077.
3. Sen S, Chakraborty R. Treatment and diagnosis of diabetes mellitus and its complication: advanced approaches. Mini-Rev Med Chem 2015;15:1132-3.
4. Fong DS, Aiello LP, Ferris FR, Klein R. Diabetic retinopathy. Diabetes Care 2004;27:2540-53.
5. Simo R, Hernandez C. Neurodegeneration in the diabetic eye: new insights and therapeutic perspectives. Trends Endocrin Met 2014;25:23-33.
6. Stem MS, Gardner TW. Neurodegeneration in the pathogenesis of diabetic retinopathy: molecular mechanisms and therapeutic implications. Curr Med Chem 2013;20:3241-50.
7. Barber AJ. A new view of diabetic retinopathy: a neurodegenerative disease of the eye. Prog Neuro-Psychoph 2003;27:283-90.
8. Lieth E, Gardner TW, Barber AJ, Antonetti DA. Retinal neurodegeneration: early pathology in diabetes. Clin Exp Ophthalmol 2000;28:3-8.
9. Jing G, Wang JJ, Zhang SX. ER stress and apoptosis: a new mechanism for retinal cell death. Exp Diabetes Res 2012;2012:589589.
10. Szegezdi E, Logue SE, Gorman AM, Samali A. Mediators of endoplasmic reticulum stress-induced apoptosis. Embo Rep 2006;7:880-5.
11. Xie Y, E J, Cai H, Zhong F, Xiao W, Gordon RE, et al. Reticulon-1A mediates diabetic kidney disease progression through endoplasmic reticulum-mitochondrial contacts in tubular epithelial cells. Kidney Int 2022;102:293-306.
12. Li J, Wang JJ, Zhang SX. Preconditioning with endoplasmic reticulum stress mitigates retinal endothelial inflammation via activation of X-box binding protein 1. J Biol Chem 2011;286:4912-21.
13. Wang M, Li Y, Li S, Lv J. Endothelial dysfunction and diabetic cardiomyopathy. Front Endocrinol 2022;13:851941.
14. Wang XZ, Ron D. Stress-induced phosphorylation and activation of the transcription factor CHOP (GADD153) by p38 MAP kinase. Science 1996;272:1347-9.
15. Gao Z, Li M, Yao F, Xia X, Duan T, Meng J, et al. Valdecoxib protects against cell apoptosis induced by endoplasmic reticulum stress via the inhibition of PERK-ATF4-CHOP pathway in experimental glaucoma. Int J Mol Sci 2022;23:12983.
16. Abcouwer SF, Gardner TW. Diabetic retinopathy: loss of neuroretinal adaptation to the diabetic metabolic environment. Ann NY Acad Sci 2014;1311:174-90.
17. Rattner A, Williams J, Nathans J. Roles of HIFs and VEGF in angiogenesis in the retina and brain. J Clin Invest 2019;129:3807-20.
18. Zeng K, Xu H, Chen K, Zhu J, Zhou Y, Zhang Q, et al. Effects of taurine on glutamate uptake and degradation in Muller cells under diabetic conditions via antioxidant mechanism. Mol Cell Neurosci 2010;45:192-9.
19. Hua YL, Ma Q, Yuan ZW, Zhang XS, Yao WL, Ji P, et al. A novel approach based on metabolomics coupled with network pharmacology to explain the effect mechanisms of Danggui Buxue Tang in anaemia. Chin J Nat Med 2019;17:275-90.
20. Zhang Y, Jiang L, Xue J, Lv M, Zhang W. The efficacy and potential mechanism of Danggui Buxue decoction in treating diabetic nephropathy: A meta-analysis and network pharmacology. Medicine 2023;102:e33481.
21. Zhang R, Han X, Huang T, Wang X. Danggui buxue tang inhibited mesangial cell proliferation and extracellular matrix accumulation through GAS5/NF-kappaB pathway. Bioscience Rep 2019;39:BSR2018174.
22. Ke HL, Zhang YW, Zhou BF, Zhen RT. Effects of Danggui Buxue Tang, a traditional Chinese herbal decoction, on high glucose-induced proliferation and expression of extracellular matrix proteins in glomerular mesangial cells. Nat Prod Res 2012;26:1022-6.
23. Ceker T, Yilmaz C, Kirimlioglu E, Aslan M. Endoplasmic-reticulum-stress-induced lipotoxicity in human kidney epithelial cells. Toxicol Res-Uk 2022;11:683-95.
24. Saint-Geniez M, Maharaj AS, Walshe TE, Tucker BA, Sekiyama E, Kurihara T, et al. Endogenous VEGF is required for visual function: evidence for a survival role on Muller cells and photoreceptors. PloS One 2008;3:e3554.
25. Li Y, Zhang F, Nagai N, Tang Z, Zhang S, Scotney P, et al. VEGF-B inhibits apoptosis via VEGFR-1-mediated suppression of the expression of BH3-only protein genes in mice and rats. J Clin Invest 2008;118:913-23.
26. Nishijima K, Ng YS, Zhong L, Bradley J, Schubert W, Jo N, et al. Vascular endothelial growth factor-A is a survival factor for retinal neurons and a critical neuroprotectant during the adaptive response to ischemic injury. Am J Pathol 2007;171:53-67.
27. Ola MS, Nawaz MI, Khan HA, Alhomida AS. Neurodegeneration and neuroprotection in diabetic retinopathy. Int J Mol Sci 2013;14:2559-72.
28. Bringmann A, Pannicke T, Grosche J, Francke M, Wiedemann P, Skatchkov SN, et al. Muller cells in the healthy and diseased retina. Prog Retin Eye Res 2006;25:397-424.
29. Toft-Kehler AK, Gurubaran IS, Desler C, Rasmussen LJ, Skytt DM, Kolko M. Oxidative stress-induced dysfunction of Muller cells during starvation. Invest Ophth Vis Sci 2016;57:2721-8.
30. Bringmann A, Wiedemann P. Muller glial cells in retinal disease. Ophthalmologica 2012;227:1-19.
31. Vecino E, Rodriguez FD, Ruzafa N, Pereiro X, Sharma SC. Glia-neuron interactions in the mammalian retina. Prog Retin Eye Res 2016;51:1-40.
32. Zhang P, Yan X, Zhang X, Liu Y, Feng X, Yang Z, et al. TMEM215 prevents endothelial cell apoptosis in vessel regression by blunting BIK-regulated ER-to-mitochondrial Ca influx. Circ Res 2023;133:739-57.
33. Zhong Y, Li J, Chen Y, Wang JJ, Ratan R, Zhang SX. Activation of endoplasmic reticulum stress by hyperglycemia is essential for Muller cell-derived inflammatory cytokine production in diabetes. Diabetes 2012;61:492-504.

Received: 10 September 2024. Accepted: 20 August 2024.

European Journal of Histochemistry 2024; 68:4140
doi:10.4081/ejh.2024.4140